Region Based Segmentation using TCRM

M. Umaselvi, E. Menaka

Abstract*: Water Resource is one of the essential supplies of the globe environment which needs to be regularly observed. There is rising need and necessitate in research of water region detection due to the unpredicted natural calamity that guide to financial, environment and individual sufferers. Assessment of water region (WR) and study on its characteristic is very fundamental step for many scheduling, particularly for country like India which made frequent changes on WR. Basically, recognize the WR from Remote sensing images is one of the impressive steps of water possessions organization for a country where it has been used superior than decades for WR detection. Techniques of WR extraction can be examine into three groups: Texture Conditional Rotation Mean (TCRM), feature extraction using TCRM algorithms, Region based segmentation. These methods, though, are of mathematical and statistical approach and little of them look at important uniqueness of multispectral image which is found on land object radiance absorption performance in every sensing spectral bands. In visible and infrared bands, the WR spectral absorption characteristics differ very much from the other earth substance. There are different data bases for the study area which consists of different form and exposure. Results show that TCRM presents adequate well detection for WR as speedy and receiving high accuracy with the suitable threshold rate.

***Keywords* : Remote sensing images, Assessment of water region, Feature extraction.**

I. INTRODUCTION

The assessment of water resources data from remote sensing by several researchers in various fields such as hydrology, oceanography, and natural science found that the environmental inaccessibility of the isolated region which causes plentiful challenge in their mapping progress. It could be hard to find because of its usual geographic arrangement. Hence, the complete preparation, revelation and analysis essential for functioning in such areas for development of the nation. Despite the fact that, most of the man made water storage dam and reservoirs are situated in mountainous zones where its topographic shadows show analogous in optical data, which is the origin for misunderstanding in the recognition and description of water. It is the most important challenge in satellite image processing.

The methods that only exploit the spectral variables derived from image pixels may be used to the most well-liked system of LULC for region, urban area, and vegetation. The recognition of very important and unimportant features is a significant element in image processing. The intensity property implemented in the segmentation process is not adequate to differentiate the water object in remotely sensed images. Accordingly, it needs derivative information of WR and which is a demanding assignment for regular clustering since its difficult textures and their properties. Subsequently study activities, away from the spectral, spatial information or the association among adjacent pixels were discover through OBIA (Csathó et al 1999) which usually get better accuracy with respect to the pixel-based approach (Myint et al 2011, Menaka & Suresh Kumar 2014, 2015) also it is preferable since WR characterize in its proper spatial landscape model as an alternative to a squared classified pixel (Blaschke & Strobl 2001). Texture features commonly used in OBIA and have been exposed to progress discrimination and segmentation accuracy (Arcidiacono et al 2012) in various land cover categories.

Some of methods execute texture analysis directly on the gray levels such as GLCM (Haralick et al 1973), autocorrelation function analysis (Lin et al 1997), Generalized Co-occurrence Matrices (GCM) (Hauta et al 1996), second order spatial averages (Gagalowicz 1988), and two-dimensional filtering in the spatial and frequency domain (Coggins & Jain 1985). The approaches rely on color image applied a single spectral band (Pesaresi & Gerhardinger 2011) that describe the spatial changeability within the bands to generate texture images. Wentz et al (2006) described that instead of choosing a single, a multiband texture could be derived from all suitable spectral bands.

Fisher et al. (2016) applied multiple water indices using multi-temporal Landsat (TM, ETM and OLI) satellite images for Automated Water Extraction Index with shadow (AWEIsh) and by no shadow (AWEInsh), Tasseled Cap Wetnes (TCWCrist) NDWI and Water Index (WI2015) and examined performance and correctness outcomes of said indices on clean and varied water pixels. Although the complication neural networks beneath the deep learning structure has been broadly used to find the objective in satellite images by categorized training sample (Isikdogan et al., 2017), limited researches have stated the demonstration of deep learning to satellite data at great scale. Wei Jiang et al., (2018) proposed the Multi-Layer Perceptron (MLP) method beneath deep learning basis to detect WR and classify image using Maximum Likelihood (ML) and water index using Landsat 8. Acharya et al. (2017) applied four different indices to Landsat 8 OLI satellite images of to Phewa Lake's. The classification with the combination of these indices, including Normalized Difference Water Index (NDWI), Modified Normalized Difference Water Index (MNDWI), Water Ratio Index (WRI), and Normalized Difference Vegetation Index (NDVI) shows better results than those of spectral bands. Therefore, this work make use of modified mean and variance algorithm as a corrective procedure to detect the dam and reservoir WR multispectral image and it

Revised Manuscript Received on April 02, 2020.
***** Correspondence Author
Dr. M. Umaselvi, Associate Professor, P. A. College of Engineering and Technology, Palladam Road, Pollachi, Coimbatore - 642002, India. umaselvisadeeskumar@gmail.com
Dr. E. Menaka*, Associate Professor, Vivekanandha College of Engineering for Women, Elayampalayam, Namakkal, Tamilnadu 642247, India. menakaparthi80@gmail.com

is illustrate in the subsequent divisions.

II. STUDY AREA

The study area is Mettur dam, which is one of the largest water storage dam constructed across the Kaveri River in Salem District, Tamil Nadu, is locating in Southern India. The area, enclosed with 76°38'46.86"E longitude, 10°07'20.86"N latitude, path 144, row 53 (data acquired on 2016/03/20) where image covers 1300 sq. Meters is showing in Figure 1. The water infinite by part of the Salem, Namakkal, Karur, Trichy, and Thanjavur are giving the asset to the Tamilnadu. The length is 1,700 meters (5,600 ft), the level of the dam is 120ft (37 meters), and the maximum capacity is 93.47 tmc. Due to lack of rainfall, the dam receives low water, and nearly goes dry during summer season (April-June). Most of the farmers and publics life is depending upon this dam water. The hotness range differ in summer from 29° C (84° F) to 37° C (99° F) and in winter 20° C (68° F) to 26° C (79° F) and an yearly usual rainfall of 812 mm.

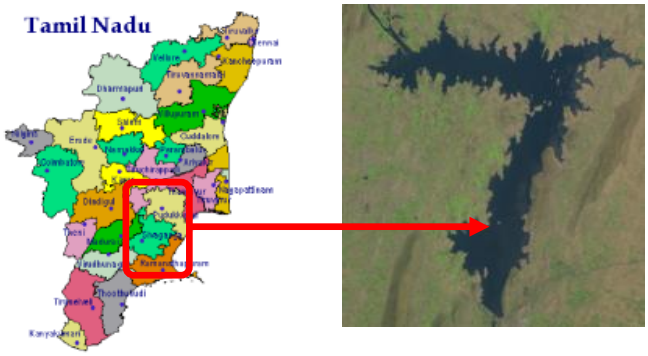

Figure 1 Study Area of Mettur Dam [Source: www.mapsofindia.com]

III. SIGNIFICANCE OF TEXTURE

The texture extraction plays an essential part in numerous techniques to detect water zones based on spatial distinction of intensity values (Akay & Aksoy2008) where it permitted the image structure mining which is not noticeable by others (Breckle & Wucherer 2006). It evaluate the variability in locale structure (Wood et al 2012) of color values between adjacent pixels in a digital image. Also it enumerates illustration characteristics of the image such as smoothness, roughness, symmetry, directionality and relationship between them. Depends on the image source, it can be considered on single or multiple bands, with all dissimilar information regarding the spatial associations of neighborhood pixels. Also, the Haralick measures on the color images provide the improved accuracy for segmentation (Menaka & Suresh Kumar 2015).

IV. RULE – BASED SEGMENTATION

The water pixels in the RS images are homogenous (uniform and flat) even though some local variability is available in brightness. The irregular water and thin water gives specular reflection and bottom reflection. Variability of atmospheric radiance, sensor gain variation and mixed pixels are the factors which affect and vary the light intensity from water (Wilson 1997). However, Haralick et al (1973) proposed texture for land-use segmentation including water, farm land, soil and urban area. Jupp et al (1985) used Root Mean Square (RMS), calculated in 3x3 windows between central and its neighboring pixels in WR given in Equation (1).

$$p(i,j) = \sum_{i=1}^{N_g}\sum_{j=1}^{N_g}(i - \mu)^2\, p(i,j) \qquad \text{eq. 1}$$

Where
p(i,j) -> spatial dependence matrix of (i,j)th entry
μ -> the mean value of the image p
Ng ->quantized distinct gray levels

Similarly variance filter (VF) defined as “local amplitude can be measured using variance” which proposed by Jain (1989) to measure uniformity of water where it calculates variance of the neighboring pixels in the n group which replaces the central pixel (Wilson 1997) is given in Equation 2.

$$S_x = \frac{1}{N-1}\sum_{i=1}^{n_1}(x_i - \bar{x})^2$$

where
N-> the number of pixels in the set
x_i->the value of pixel i
$\bar{x}$->the mean of neighboring pixel values

Some of the data values are affected by neighbor goods when applying VF due to the causes of external factors. Thus it leaves a few WR as unclassified which is very much necessary to segment its boundaries between vegetation, rock, sand, and soil. So, the new modified feature extraction algorithm proposed in the next section.

V. TEXTURE CONDITIONAL ROTATION VARIANCE (TCRV)

The proposed TCRV algorithm is used for extraction which eliminates the limitations of VF. It is developed based on Conditional Rotation and Variance where the condition is set by the manual input which selects the pixels to calculate the variance value of the image in 3x3 and 5x5 windows. The center pixel called as Region of Interest (RoI) which set as an origin point to rotate the window shown in Figure 2.

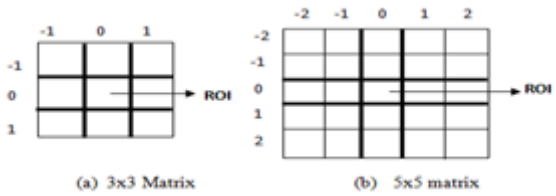

Figure 2 TCR Pixel Positions

The RoI is replaced by the variance value of 8 pixels and the resultant value produces the textured image using the Equation 3 & 4.

$$I(i,j) = \frac{1}{8}\sum_{i=-1}^{1}\sum_{j=-1}^{1}(I(i,j) - c\mu)^2$$

where $c\mu = \frac{1}{8}\sum_{i=-1}^{1}\sum_{j=-1}^{1} I(i,j)$

i=0,j<0 : L
i=0,j>0 : R
i<0,j=0 : U
i>0,j=0 : L_O
i<0,j<0 : UL
i<0,j>0 : UR
i>0,j<0 : L_OL
i>0,j>0 : L_OR

eq.3

$$c\mu = (I(i-1,j-1)+I(i-1,j)+I(i-1,j+1)+I(i,j-1)+I(i,j+1)+ I(i+1,j-1)+I(i+1,y)+I(i+1,j+1))/8$$

eq.4

where I(i,j) -> image pixel
$c\mu$ ->conditional mean value

It is a three phase process. First, conditional mean value calculated using 8 pixels of RoI which are selected by applying TCR. Secondly the mean is subtracted from each surrounding values and summed up its variance called Conditional Rotation Variance (CRV). Finally, the RoI replaced by CRV value.

VI. TEXTURE CONDITIONAL ROTATION MEAN (TCRM)

It is developed based on the conditional rotation and mean where the condition is set by manual which selects the pixels to calculate the mean value of the image. The dimension of the sliding window takes account of the sufficient and essential for WR which manipulates the accuracy. Thus, the option of sub-window is a vital step with different resolutions, texture parameters and its expressions. Therefore, there is a need to select suitable size. In this proposed method, two kinds of sliding windows 3x3 and 5x5 applied for feature extraction. The derivative gives eight new algorithms which are directional oriented such as Diagonal (D), Horizontal (Left – L, Right - R), Vertical (Upper - U, Lower - Lo) and its combinations of 3x3 which shows in Equation 5 to 11.

DIA

$$I(i,j) = \frac{1}{4}\sum_{i=-1}^{1}\sum_{j=-1}^{1} I(i,j)$$

i<0,j<0 : UL
i<0,j>0 : UR
i>0,j<0 : L_oL
i>0,j>0 : L_oR

eq.

LR

$$I(i,j) = \frac{1}{2}\sum_{j=-1}^{1} I(i,j)$$

i=0,j<0 : L
i=0,j>0 : R

eq. 6

LRD

$$I(i,j) = \frac{1}{6}\sum_{i=-1}^{1}\sum_{j=-1}^{1} I(i,j)$$

i=0,j<0 : L
i=0,j>0 : R
i<0,j<0 : UL
i<0,j>0 : UR
i>0,j<0 : L_oL
i>0,j>0 : L_oR

eq. 7

UL_o

$$I(i,j) = \frac{1}{2}\sum_{i=-1}^{1} I(i,j)$$

i<0,j=0 :U
i>0,j=0 : L_o

eq. 8

UL_oD

$$I(i,j) = \frac{1}{6}\sum_{i=-1}^{1}\sum_{j=-1}^{1} I(i,j)$$

i<0,j=0 : U
i>0,j=0 : L_o
i<0,j<0 : UL
i<0,j>0 : UR
i>0,j<0 : L_oL
i>0,j>0 : L_OR

eq. 9

$LRUL_o$

$$I(i,j) = \frac{1}{4}\sum_{i=-1}^{1} I(i,j)$$

i=0,j<0 : L
i=0,j>0 : R
i<0,j=0 : U
i>0,j=0 : L_o

eq. 10

$LRUL_o$D

$$I(i,j) = \frac{1}{8}\sum_{i=-1}^{1}\sum_{j=-1}^{1} I(i,j)$$

i=0,j<0 : L
i=0,j>0 : R
i<0,j=0 : U
i>0,j=0 : L_o
i<0,j<0 : UL
i<0,j>0 : UR
i>0,j<0 : L_oL
i>0,j>0 : L_oR

eq. 11

Where I(i,j) represents image pixel
DIA-Diagonal, LR-Left Right, LRD-Left Right Diagonal, UL_o-Upper Lower, UL_oD-Upper Lower Diagonal, $LRUL_o$- Left Right Upper Lower, $LRUL_o$D-Lower Right Upper Lower Diagonal.

The TCRM using D considered 4 pixels of RoI. The LR and UL processed with 2 pixels each and 6 pixels taken for the combination of D with UL and LR. The mean calculated and it replaces the RoI according to the derivatives. TCRM using LRULD 5x5 window pixel positions are shown in Equation 12 & 13.

$$I(i,j) = \frac{1}{24}\sum_{i=-2}^{2}\sum_{j=-2}^{2} I(i,j)$$

eq. 12

I(x,y) = (I(x-2,y-2)+I(x-2,y-1)+I(x-2,y)+I(x-2,y+1)+ I(x-2,y+2)+I(x-1,y-2)+I(x-1,y-1) +I(x-1,y)+I(x-1,y+1)+ I(x-1,y+2)+I(x,y-2)+I(x,y-1)+I(x,y+1)+I(x,y+2)+ I(x+1,y-2)+I(x+1,y-1)+I(x+1,y)+I(x+1,y+1)+ I(x+1,y+2)+I(x+2,y-2)+I(x+2,y-1)+I(x+2,y)+ I(x+2,y+1) +I(x+2,y+2))/24

eq. 13

where I(x,y) -> image pixel
x,y -> row and column values of I.

VII. RESULT AND DISCUSSION

This study presents a root for prudent water organization of large basins. Civilization around the world has long fought with the planning and management of WR with growing populations, resource uses, ecosystem degradation and climate change where the decisions can reduce the impacts of geologic scale. Extraction of WR from SAR images using thresholding, noise removal, SAR amplitude and terrain information produces the overall accuracy of 96.48% after differentiating the misclassified segments, while amplitude detail alone produces only 83.67%. Hence, the proposed algorithm provides the right result on different Landsat 8 images of dam and reservoirs.

The occurrence of WR determined by TCR which explained in the sub section 5. It produces coarse image and applied multiresolution segmentation with varying threshold to splits the water area from various objects such as forest, land, rock and sandy regions for precise results. The following Equations 14 & 15is used to test the accuracy and fault tolerance:

$$\text{Segmentation Accuracy} = \frac{\text{Segmented water pixels by the algorithm}}{\text{Sample Image water pixels}} \quad \text{eq.14}$$

$$\text{Fault Tolerance} = \frac{\text{Missed water pixels by the algorithm}}{\text{Sample Image water pixels}} \quad \text{eq.15}$$

The results of WR using 11 algorithms with a threshold of 225 for Mettur dam is shown in Figure 3 and Table 1. The sample outputs ant its accuracies are shown in Figure 4 and Table 2-3. The yellow boundary is the objective WR which obtained by proposed methods and green is the other land uses. It acquires good results except in areas near to the dense forest and wetland where pixels could not well segregated. The notable one is that the small WR covered by hill or rock and small land covered by WR also well processed.

HKM, DIA and LRULD 5X5produces over segmentation i.e., the mountain shadow and dense forest boundaries are recognized as WR due to its backscattered values. Also, HKM forms many inner clusters within WR.ULD is not entirely cover the overall WR and it splits WR into groups which includes wetland and other Land objects. LRUL performs same as LR which ignores the slant WR in the corner region. LRULD using 5x5 removes the non-water area entirely which covers only WR where it includes non WR as water. HKV creates many groups like ULD and left the few WR as non water. LRULD 3x3 obtained the exact WR and achieved high accuracy. To analyze this work, 100 subsets created from 7 different locations in India where the LRULD 3x3 reached overall accuracy of 98.96% with fault tolerance of 1.03% is shown in Table 1. The running time also considerably less compared to other algorithms.

VIII. CONCLUSION

The work carried out in this study presents a new technique for detecting and extracting the specific WR which observe the status of water resources fast and timely which affords enormous instant impact for protecting the surroundings and attains sustainable growth. A meticulous examination has been specified since its accurate surveying is extremely significant for Central Water Commission where the methodologies found valuable to take precautionary actions against water scarcity and flood which facilitates to improve the correctness in the RS lake, river and reservoir. TCRM gives enough fine position for extracting WR as fast and getting high precision with the appropriate threshold value. Also, this proposed work may be integrated with other algorithms such as TCR Haar Wavelet and Hard clustering.

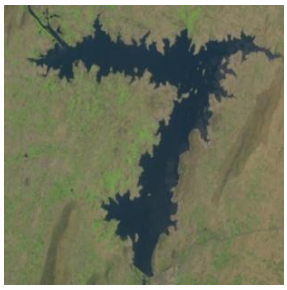

a)

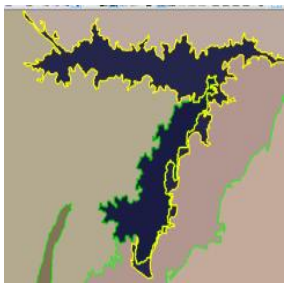

b)

c)

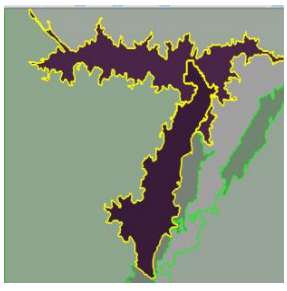

d)

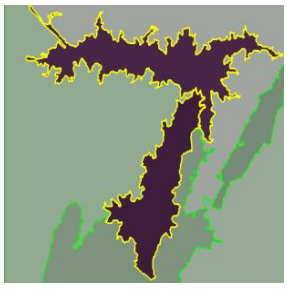

e)

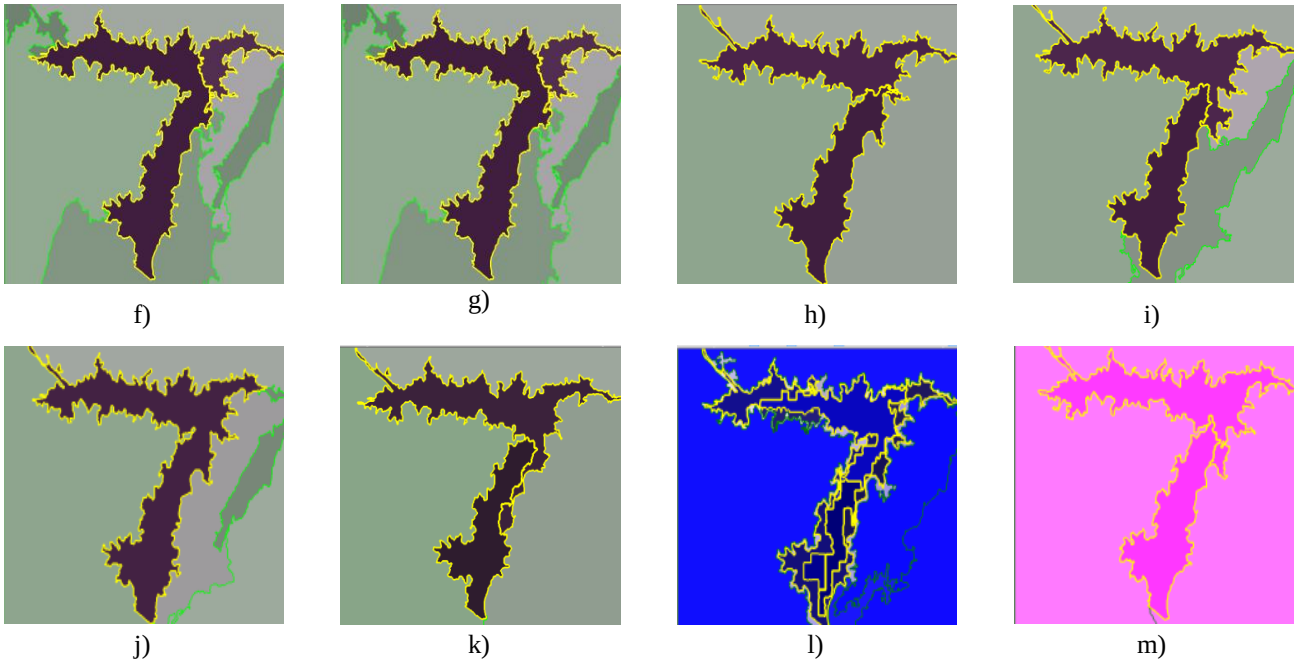

Figure 3 TCR Resultant Images of Mettur Dam, a) Original Image, b) Multiresolution Segmentation Image, c) HKM image, d) DIA image, e) LR image, f) LRD image, g) UL image, h) ULD image,i)LRUL image, j)LRULD 3x3 image, k)LRULD 5x5 image, l)HKV image, m)TCRV image

Table 1 Accuracy Analysis of Mettur Dam

Algorithms	Accuracy %	FT %	RT in Sec.
HKM	104.2574*	-4.25744	95.47682
DIA	98.30153	1.698466	42.31791
LR	93.636	6.364	26.06791
LRD	94.0876	5.912402	35.84285
UL_o	97.27182	2.728181	30.52501
UL_oD	97.59572	2.40428	56.37228
$LRUL_o$	98.92516	1.074836	66.31515
$LRUL_oD$ 3X3	99.90723	0.092769	10.00709
$LRUL_oD$ 5X5	93.53487	6.465128	74.96019
HKV	87.73688	12.26312	96.0465
TCRV	96.79	3.210004	87.6861

*-> Over segmentation, FT->Fault Tolerance, RT->Running Time

Image Name	MR	HKM	HKV	TCRV with LRULD 3x3	TCRM with LRULD 3x3
U41	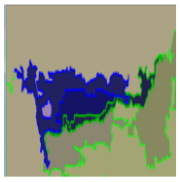	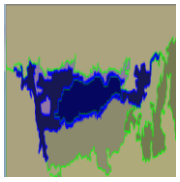	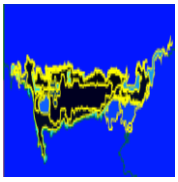		
U42	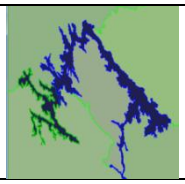	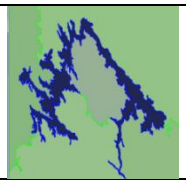	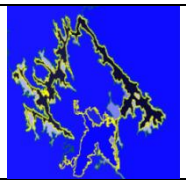	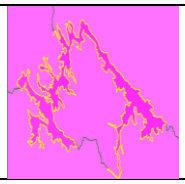	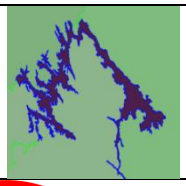

U43	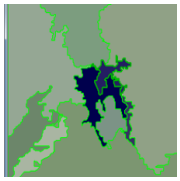	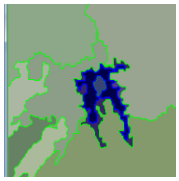	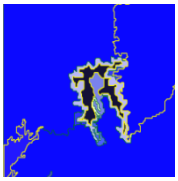	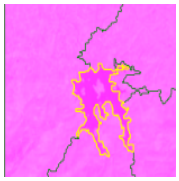	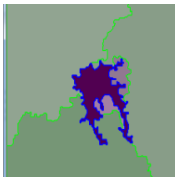
U44		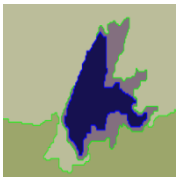	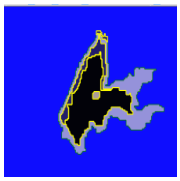		
U45	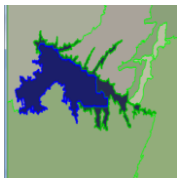	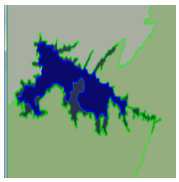	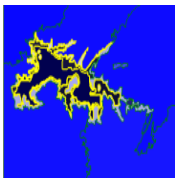	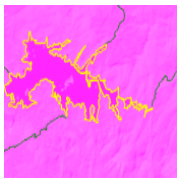	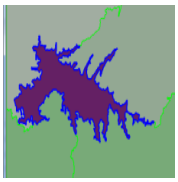
U46	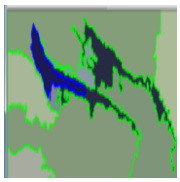	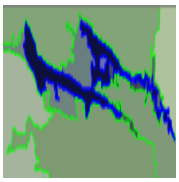	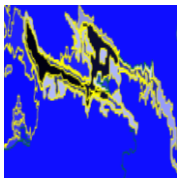		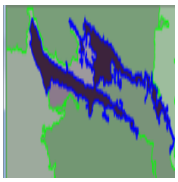
U47		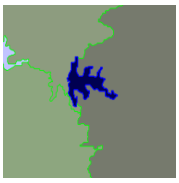	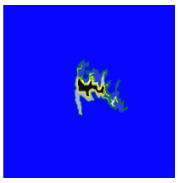	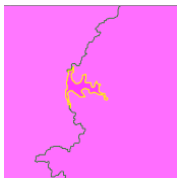	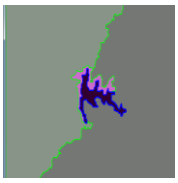
U48			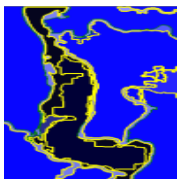	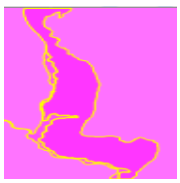	

Figure 4 Resultant Images of Region based Segmentation using TCR

Image Name	MR	HKM	HKV	TCRV with LRULD 3x3	TCRM with LRULD 3x3
U49	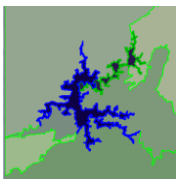	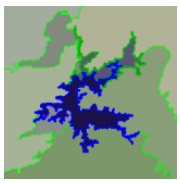	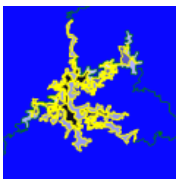	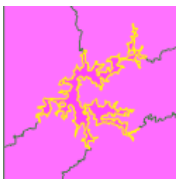	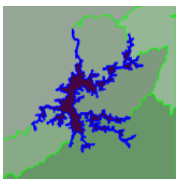
U50			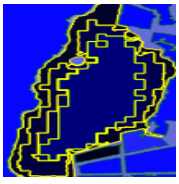		
U51					

U52	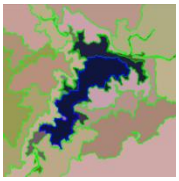	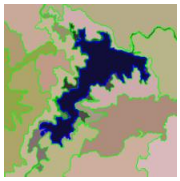	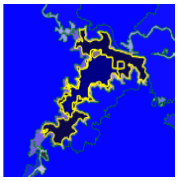	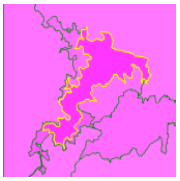	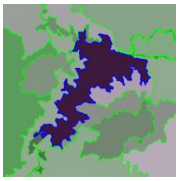
U53	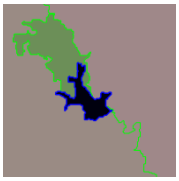	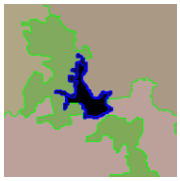	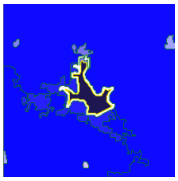		
U54		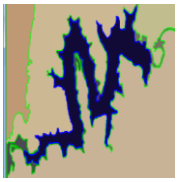	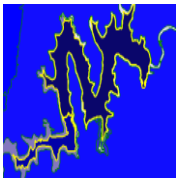		
U55	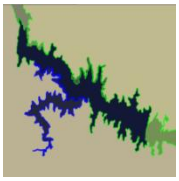	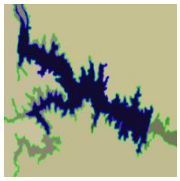	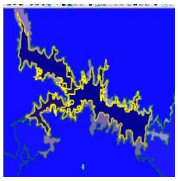	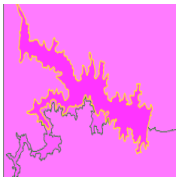	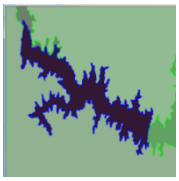
U57			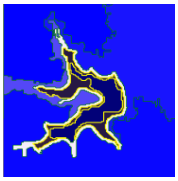	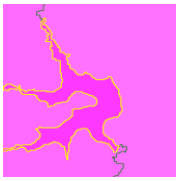	
U58	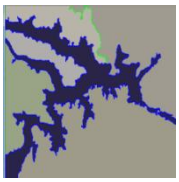		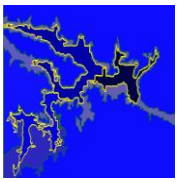	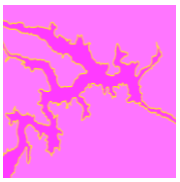	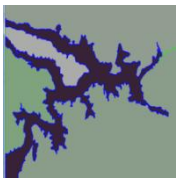

Image Name	MR	HKM	HKV	TCRV with LRULD 3x3	TCRM with LRULD 3x3
U59		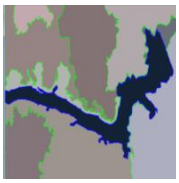	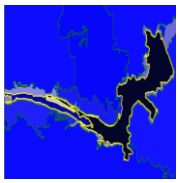	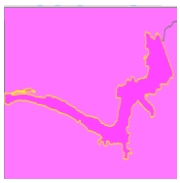	
U60	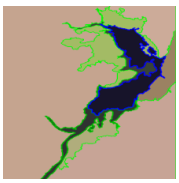	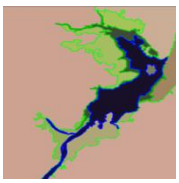	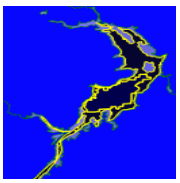	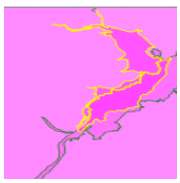	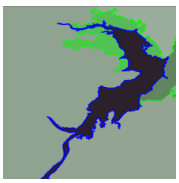
U61					

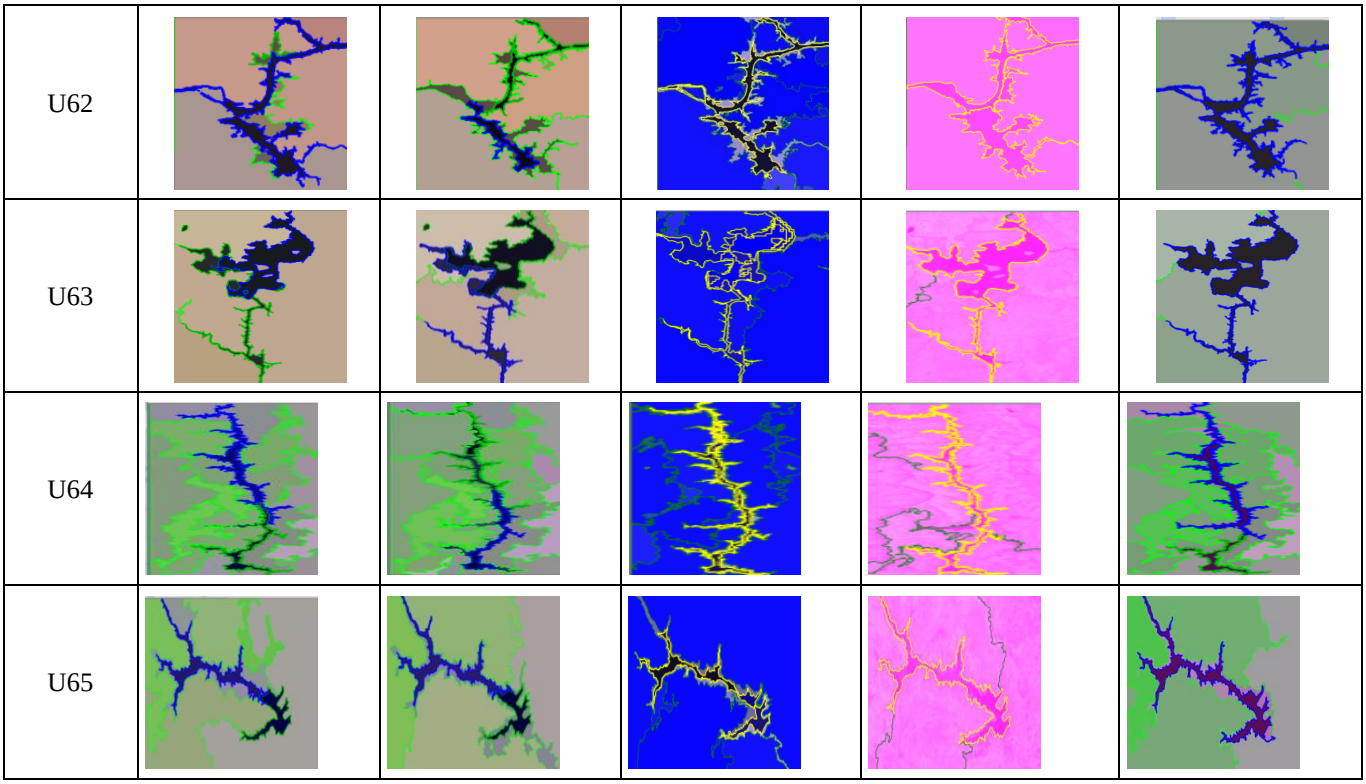

Table 2 Performance Evaluation of Region based Segmentation using TCRM5

Image Name	Image Dimension	Threshold	Water Pixels	Percentage of Water Region using					
				MUL	Existing		TCRM 3x3		
					HKM	HKV	DIA	LR	LRD
U41	770x240	140	31410	91.8465	104.8	75.8898	90.5985	92.2859	91.0124
U42	810x515	280	49228	97.5441	106.22	74.9411	96.8575	96.4228	95.5249
U43	220x200	60	2730	101.978	116.74	55.9341	102.308	81.538	103.443
U44	176x126	130	2782	96.9446	135.37	71.6751	88.0661	98.059	94.3206
U45	500x345	135	22602	101.115	105.1	76.2764	117.538	101.491	96.9206
U46	479x153	95	9735	98.2948	116.56	53.4977	123.297	99.2912	97.6168
U47	283x236	80	1210	73.3058	129.59	39.0909	111.322	93.5537	94.2975
U48	280x496	160	38905	102.356	127.33	130.223	105.046	104.28	105.275
U49	350x340	115	8574	103.989	146.59	53.8022	102.344	105.563	99.9883
U50	325x528	255	89442	84.136	113.59	70.91416	85.767	80.694	82.615
U51	198x276	111	17161	94.773	109.67	83.9928	91.2534	108.921	95.2334
U52	480x430	125	25564	107.53	104.98	80.68018	111.919	82.461	107.405
U53	200x200	95	1526	88.1389	110.03	67.3657	99.0826	87.3526	81.659
U54	520x350	245	38481	103.849	108.8	110.961	95.7641	98.5395	101.097
U55	655x475	225	52955	90.9848	108.34	78.461	89.4042	92.2859	88.6715
U56	625x510	225	62056	81.25	104.26	87.7369	98.3015	93.636	94.0876
U57	170x190	135	4111	99.8541	115.37	76.2102	98.6865	95.0377	98.7351
U58	740x510	355	77388	104.935	99.67	66.0025	98.225	104.021	82.977
U59	810x500	340	59999	110.294	101.54	78.3663	102.472	96.6849	97.405
U60	740x1050	340	99918	100.136	124.09	76.865	112.199	97.0936	95.116
U61	432x745	400	65842	100.808	103.37	62.1184	105.411	98.6452	97.0687
U62	576x601	255	42992	99.758	114.16	63.9584	99.7558	104.161	102.533
U63	1004x1356	470	190042	98.9266	104.36	67.4467	98.2946	98.5551	98.5551
U64	555x1260	220	56053	88.1327	108.96	77.391	117.014	99.2781	81.829
U65	600x425	205	18290	93.7132	92.76	64.6513	84.803	92.6987	86.1864
Average %				**96.58372**	**112.49**	**73.77807**	**101.0292**	**96.102**	**94.78292**

Table 3 Performance Evaluation of Region based Segmentation Using TCRM

Image Name	Image Dimension	Threshold	Water Pixels	Percentage of Water region using					
				TCRM 3x3				TCRV 3x3	TCRM 5x5
				UL	ULD	LRUL	LRULD	LRULD	LRULD
U41	770x240	140	31410	82.3114	91.9675	93.6581	98.7743	91.6301	91.4581
U42	810x515	280	49228	98.0844	95.2385	98.0296	99.7806	105.639	93.8917
U43	220x200	60	2730	101.099	119.451	106.337	99.5971	90.421	111.136
U44	176x126	130	2782	95.6866	96.2257	95.2552	90.0072	101.186	98.8857
U45	500x345	135	22602	97.3896	78.065	100.168	99.7965	102.571	104.115
U46	479x153	95	9735	94.9563	96.0041	95.6959	99.6405	107.673	116.014
U47	283x236	80	1210	91.5702	80.0826	84.3802	99.3388	69.0083	81.2397
U48	280x496	160	38905	99.691	129.384	99.71	99.8458	101.223	105.223
U49	350x340	115	8574	90.8444	101.201	100.023	106.158	107.756	98.6704
U50	325x528	255	89442	81.75	83.225	86.761	98.2469	95.6508	90.02
U51	198x276	111	17161	95.9676	96.0783	94.8022	97.3953	92.0343	101.573
U52	480x430	125	25564	105.328	105.422	103.802	95.9905	89.2701	106.76
U53	200x200	95	1526	92.6606	95.675	99.6723	98.3617	101.376	112.975
U54	520x350	245	38481	96.0162	96.1799	96.8894	96.8946	95.8395	93.8385
U55	655x475	225	52955	89.2135	86.0466	87.191	87.3326	86.8209	91.2756
U56	625x510	225	62056	97.2718	97.5957	98.9252	99.907	96.79	93.5349
U57	170x190	135	4111	105.108	94.9404	91.1457	97.9081	100.268	98.4919
U58	740x510	355	77388	103.032	94.3919	98.2943	97.855	96.7747	98.943
U59	810x500	340	59999	104.44	97.9916	99.0183	96.9766	86.6231	106.557
U60	740x1050	340	99918	97.9123	97.7241	97.7021	98.0904	83.2573	104.691
U61	432x745	400	65842	97.1568	99.4882	105.05	99.0462	70.7101	92.9437
U62	576x601	255	42992	82.068	96.1132	104.752	105.147	92.378	123.342
U63	1004x1356	470	190042	98.2783	97.3195	99.3359	99.1328	100.491	101.421
U64	555x1260	220	56053	94.1716	79.445	90.8212	98.319	94.0342	105.79
U65	600x425	205	18290	91.9557	86.1864	85.6228	114.562	119.65	85.53
Average %				**98.39853**	**100.4577**	**98.5617**	**98.96418**	**97.24302**	**100.3328**

REFERENCES

1. Acharya, T. D., Subedi, A., Yang, I. T., & Lee, D. H., 2017. Combining Water Indices for Water and Background Threshold in Landsat Image. In Multidisciplinary Digital Publishing Institute Proceedings, 2(3), 143.
2. Akay, HG & Aksoy, S 2008, 'Automatic detection of geospatial objects using multiple hierarchical segmentations', IEEE Transactions on Geoscience and Remote Sensing, vol. 46, no.7, pp. 2097-2111.
3. Arcidiacono, C, Porto, SMC &Cascone, G 2012, 'Accuracy of crop-shelter thematic maps: a case study of maps obtained by spectral and textural classification of high-resolution satellite images', Journal of Food Agricculture Environment, vol. 10, pp.1071–1074.
4. Blaschke, T &Strobel, J 2001, 'What's wrong with pixels? some recent developments interfacing remote sensing and GIS', Proceeding of GIS – Zeitschriftfür Geo informations system, Hüthig GmbH & Co. KG Heidelberg, pp. 12-17.
5. Breckle, SW & Wucherer, W 2006, '16 vegetation of the pamir (tajikistan): land use and desertification problems in land use change and mountain biodiversity', Taylor & Francis, Boca Raton, FL, USA, pp. 225–237.
6. Coggins, JM & Jain, AK 1985, 'A spatial filtering approach to texture analysis', Pattern Recognition Letters, pp. 195-203.
7. Csathó, B, Schenk, T, Lee, DC & Filin, S 1999, 'Inclusion of multispectral data into object recognition', International Archives of the Photogrammetry, Remote Sensing Spatial Information Science, vol. 32, pp. 53–61.
8. Fisher, A, Flood, N, & Danaher, T, 2016, 'Comparing Landsat water index methods for automated water classification in eastern Australia', Remote Sensing of Environment, vol. 175, pp. 167-182.
9. Gagalowicz, A 1988, 'Blind texture segmentation', Proceding of the 9th International Conference on Pattern Recognition, pp. 46-50.
10. Haralick, RM, Shanmugam, K &Dinstein, I 1973, 'Texture for image classification', IEEE Transaction Systems Man Cybernet, vol.3, no.3, pp. 610–621.
11. Hauta - Kasari, M, Parkkinen, J, Jaaskelainen, T & Lenz, R 1996, 'Generalized cooccurrence matrix for multispectral texture analysis', Proceding of the 13th International Conference on Pattern Recognition, pp. 785-789.
12. Isikdogan, F., Bovik, A.C. and Passalacqua, P., 2017. Surface Water Mapping by Deep Learning. Ieee Journal of Selected Topics in Applied Earth Observations and Remote Sensing,10(11) ,pp.17-28.
13. Jain, AK 1989, 'Fundamentals of digital image processing, Prentice Hall, Englewood Cliffs, New Jersey.
14. Jupp, DLB, Mayo, KK, Kuchler, DA, Heggen, SJ, Kendall, SW B.M. Radke, BM &Ayling, T 1985, 'Landsat based interpretation of the cairns section of the great barrier reef marine park', Australia Commonwealth Scientific & Industrial Research Organization Division of Water & Land Resources Natural Resources Series (4), pp. 1-51
15. Lin, HC, Wang, LL &Yang, SN 1997, 'Extracting periodicity of a regular texture based on autocorrelation functions', Pattern Recognition Letters, vol. 18, no. 5, pp. 433-443.
16. Menaka, E & Suresh Kumar, S, "Analysis Deforestation Using Threshold Based Clustering Algorithm", International Journal of Applied Engineering Research 9 (23), 21031-21054, 2014.
17. Menaka, E & Suresh Kumar, S, "Improving segmentation accuracy for detecting deforestation using texture feature derived from Landsat 8 OLI multispectral imagery", European Journal of Remote Sensing, Vol.48, pp.169-181, 2015.
18. Myint, SW, Gober, P, Brazel, A, Grossman-Clarke, S & Weng, Q 2011, 'Per-pixel vs. object-based classification of urban land cover extraction using high spatial resolution imagery', Remote Sensing Environment, vol. 115, pp. 1145–1161.
19. Pesaresi, M & Gerhardinger, A 2011, 'Improved textural built-up presence index for automatic recognition of human settlements in arid regions with scattered vegetation', IEEE Journal Selecting Topics in Applied Earth Observing Remote Sensing, vol. 4, pp. 16–26.
20. Wei Jiang, Guojin He, Tengfei Long, Yuan Ni 2018, 'Detecting water bodies in Landsat 8 OLI image using deep learning', The International Archives of the Photogrammetry, Remote Sensing and Spatial Information Sciences, vol. 43 (3), pp. 669-672.
21. Wentz, EA, Stefanov, WL, Gries, C & Hope, D 2006, 'Land use and land cover mapping from diverse data sources for an arid urban environments', Computing Environment Urban System vol. 30, pp. 320–346.

22. Wilson, PA 1997, 'Rule-based classification of water in landsat MSS images using the variance filter, Photogrammetric Engineering & Remote Sensing, vol. 63, no. 5, pp. 485 - 491.
23. Wood, EM, Pidgeon, AM, Radeloff, VC, Keuler, NS 2012, 'Image texture as a remotely sensed measure of vegetation structure', Remote Sensing Environment, vol. 121, pp. 516–526.

AUTHORS PROFILE

Dr. M. Umaselvi - has received B.E CSE and M.E CSE in 2002 and 2006respectively. She has pursued her Ph.D. (Image Processing, 2019) from Anna University, Chennai. Presently she is working as Associate Professor in Dept. of CSE, P.A College of Engineering and Technology, Coimbatore, Tamil Nadu, India. She has academic experience of 10 years and she has presented papers in five International Journals, four International conferences and six National conferences in various fields. She is a Member of Institute of Research Engineers and Doctors (IRED), International Association of Engineers (IAENG). Her areas of interest are Satellite image processing and analysis, pattern recognition and Wireless Sensor Networks.

Dr. E. Menaka - has received B.E CSE and M.E CSE in 2002 and 2006 respectively. She has pursued her Ph.D. (Image Processing, 2017) from Anna University, Chennai, Tamil Nadu. Presently she is working as Associate Professor in Dept. of CSE, Vivekanandha College of Engineering for Women, Namakkal, Tamil Nadu, and India. She has academic experience of 15 years and she has presented papers in 25 International Journals, 18 International Conferences and 13 National Conferences in various fields. She is a Member of IET, IAENG, SAGE, CSE and ISSE. Her areas of interest are Satellite image processing & analysis and Wireless Sensor Networks.